

## **Highlights**

- The paper does an overview of the literature available for Guidance and Control applied to In-orbit Servicing and Assembly that is common in the space industry.
- Along with a literature review, the document collects recent approaches and techniques that are promising to tackle some of the issues of GNC in future missions.
- Lastly, the solutions being researched in the academy and companies in the sector for the Active Debris Removal problem are highlighted to point practitioners towards a complete view of the field.

# Guidance and Control for In-Orbit Servicing and Assembly Missions

Daniel Silvestre<sup>a,b</sup> and Pedro Lourenço<sup>c</sup>

<sup>a</sup>School of Science and Technology, NOVA University of Lisbon, Largo da Torre, 2829-516 Caparica, Portugal

<sup>b</sup>COPELABS, Lusófona University, Campo Grande 376, 1749-024 Lisbon, Portugal

<sup>c</sup>GMV, Alameda dos Oceanos no. 115, 1990-392 Lisbon, Portugal

© 20xx Elsevier Ltd. All rights reserved.

Chapter Article tagline: update of previous edition,, reprint..

**Keywords:** Close-range Maneuvers, Control Barrier Functions, Control Lyapunov Functions, Far-range Maneuvers, Guidance, Navigation and Control, In-orbit Servicing and Assembly, Model Predictive Control, Optimal Control, Optimization-based Controllers, Reachability Analysis, Rendezvous, Trajectory Optimization

## Glossary

<b>AOCS</b>	Attitude and Orbit Control System
<b>DDVV</b>	Design, Development, Verification & Validation
<b>GNC</b>	Guidance, Navigation, and Control
<b>ESA</b>	European Space Agency
<b>IOA</b>	In-orbit Assembly
<b>IOS</b>	In-orbit Servicing
<b>MIP</b>	Mixed Integer Programming
<b>MPC</b>	Model Predictive Control
<b>NASA</b>	National Aeronautics and Space Administration
<b>OSAM</b>	On-orbit Servicing, Assembly, and Manufacturing
<b>QP</b>	Quadratic Programm
<b>LVLH</b>	Local Vertical Local Horizontal

## Abstract

In-orbit servicing (IOS) and in-orbit assembly (IOA) missions are becoming increasingly vital for the maintenance and expansion of space infrastructure. Effective Guidance Navigation and Control (GNC) systems are essential for these missions, ensuring precise maneuvering and stability of spacecraft. Traditional GNC methods, though effective, often fall short in adapting to the dynamic and complex nature of IOS and IOA missions. This paper surveys the field of GNC for space applications, focusing on the emerging trend of optimization-based controllers as a replacement for traditional methods. We cover the various challenges associated with IOS and IOA, delve into the dynamic models of spacecraft, including orbital mechanics, attitude kinematics, and dynamics, and discuss the impact of internal and external disturbances. The paper then explores commonalities in far-range and close-range interactions, presenting design models, literature reviews, and identifying areas for further research. Special attention is given to the close proximity operations required for IOS and IOA, with a detailed examination of design models, current literature, and the unique challenges faced. Optimization-based controllers, particularly Model Predictive Control (MPC) and Convex Optimization techniques like Quadratic Programs (QPs) based on Control Lyapunov Functions (CLFs) and Control Barrier Functions (CBFs), are highlighted for their potential to enhance the performance and adaptability of GNC systems in these complex missions.

## 1 Introduction

In-orbit servicing and assembly missions represent a transformative shift in space operations, where satellites and space structures are maintained, repaired, upgraded, or even assembled directly in orbit. These missions aim to extend the operational life of existing satellites, construct large space telescopes or habitats, and support sustainable space exploration and utilization. By enabling on-site repairs and upgrades, these missions can significantly reduce the need for launching replacement satellites, thereby saving costs and resources. Furthermore, the ability to assemble large structures in space, which would be impossible to launch in one piece due to size constraints, opens new horizons for scientific exploration, commercial endeavors, and even human habitation in space.

Guidance Navigation and Control (GNC) systems are the backbone of these sophisticated missions. GNC encompasses the technologies and algorithms that allow spacecraft to autonomously determine their position and orientation, plan precise trajectories, and execute maneuvers necessary for close-proximity operations, such as docking, berthing, or capturing a satellite. The precision and reliability of GNC systems are critical, as even minor deviations can lead to mission failure or catastrophic collisions. Effective GNC systems ensure that servicing vehicles can approach and interact with target satellites safely and efficiently, and that assembly missions can accurately position components to construct large structures in the harsh environment of space.

Advancements in GNC technology are essential for the success and future development of in-orbit servicing and assembly missions.

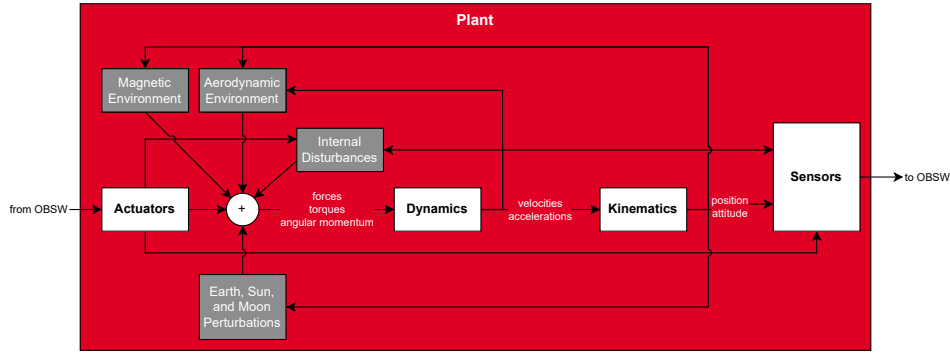


Fig. 1 High-level block diagram of the space environment control plant.

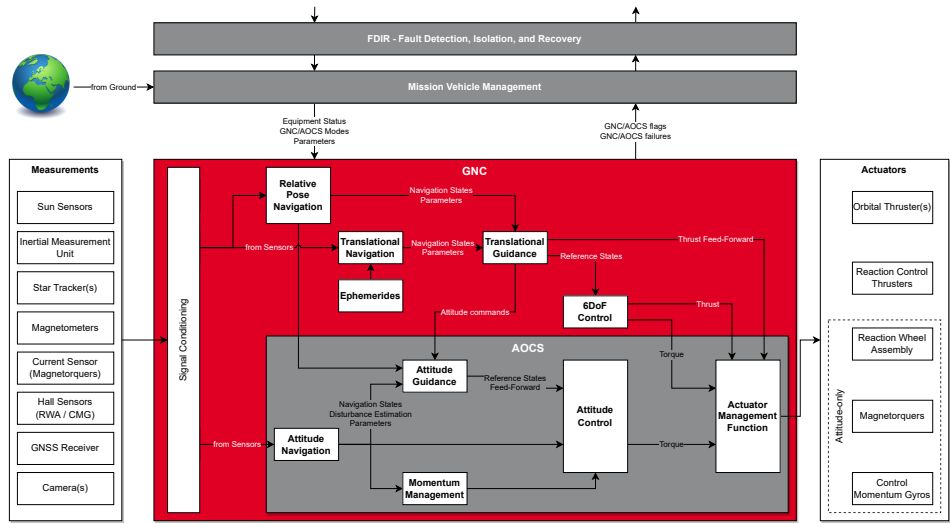


Fig. 2 A typical GNC/AOCS architecture for formation flying and proximity operations, not including the manipulator control system.

Traditional GNC methods, while robust, often lack the flexibility and adaptability required for these complex operations. Emerging trends in optimization-based controllers and autonomous systems offer promising solutions to these challenges. These advanced techniques can enhance the precision of maneuvers, optimize fuel usage, and enable real-time decision-making capabilities, which are crucial for handling the uncertainties and dynamic conditions encountered in space.

The potential benefits of effective GNC in Attitude and Orbit Control System (AOCS) systems are profound. By enhancing the capability and reliability of in-orbit servicing and assembly missions, advanced GNC technologies can contribute to the sustainability and expansion of space infrastructure. This includes reducing the frequency and cost of launches, minimizing space debris by extending the life of satellites, and facilitating the construction of large-scale space habitats and research facilities. Ultimately, these advancements support a more resilient and versatile space ecosystem, paving the way for future exploration and exploitation of space resources, and potentially transforming our approach to space operations and infrastructure development.

### 1.1 Guidance, Navigation and Control for Space Applications

Spacecraft vehicles can be modeled by a set of differential equations corresponding to the dynamics, which are driven by the forces, torques and angular momentum caused by the gravitational, magnetic, and aerodynamic environment, internal disturbances, actuators actions and perturbation from celestial bodies. As illustrated in Fig. 1, the velocities and accelerations then change the position and attitude of the spacecraft through the kinematics equation. We then require sensors to obtain estimates from these signals in order to decide which values should be applied to the actuators. This mapping of state variables to actuators variables will be performed at the GNC/AOCS subsystem.

A typical GNC/AOCS architecture for formation flying and proximity operations involves a comprehensive integration of various sensors, actuators, and computational modules, ensuring precise control and coordination between multiple spacecraft. This architecture is critical for missions where spacecraft need to maintain a specific formation or execute close-proximity maneuvers, excluding the manipulator control systems.

As illustrated in Fig. 2, the architecture includes several key components and processes. The GNC system is in charge of receiving measurements from sun sensors, Inertial Measurement Units (IMUs), star trackers, magnetometers, magnetorquers, hall sensors, Global

#### 4 Guidance and Control for In-Orbit Servicing and Assembly Missions

Navigation Satellite System (GNSS) receivers and cameras to determine the state variables for the spacecraft. This data feeds into the navigation subsystem, which estimates the spacecraft's position, velocity, and attitude. Navigation states and disturbance estimations are derived from this sensor data, allowing the system to understand the spacecraft's dynamics accurately.

The guidance subsystem uses reference states and mission parameters to compute the desired trajectories and attitudes. It includes translational and attitude guidance modules, which generate the necessary commands to achieve the mission objectives. These commands are then processed by the control subsystem, which consists of attitude control, momentum management, and actuator management functions. This subsystem ensures that the spacecraft follows the computed trajectories and maintains the desired attitude, using actuators like reaction control thrusters, reaction wheel assemblies, magnetorquers, and control momentum gyros.

To maintain the system reliability and safety, the GNC/AOCS architecture includes Fault Detection, Isolation, and Recovery (FDIR) mechanisms at system, software, sensor, and actuator levels. Another task is the mission vehicle management overseeing the overall system operation integrated with the ground control, coordinating between different subsystems and ensuring that all components function correctly. This architecture is designed to be robust and adaptive, capable of handling the complex and dynamic environment of space, ensuring successful formation flying and proximity operations.

In Fig. 2, the controllers inside the GNC block calculate thrust and torques to achieve the reference values. Lastly, the AOCS block can possess low-level controllers for the attitude as well as an actuator management system that converts the control actions in the actual values for each actuator. The available actuators for translational motion are typically the orbital and reaction thrusters. The latter are also useful for slew manoeuvres (large scale re-orientation), but do not allow efficient precise attitude control. For that purpose, the vehicle can possess reaction wheels, magnetorquers and momentum gyros allowing small attitude corrections. Given the high investment around maintaining a spacecraft, it is also essential that the software is correctly implementing all the required functions from the identified blocks.

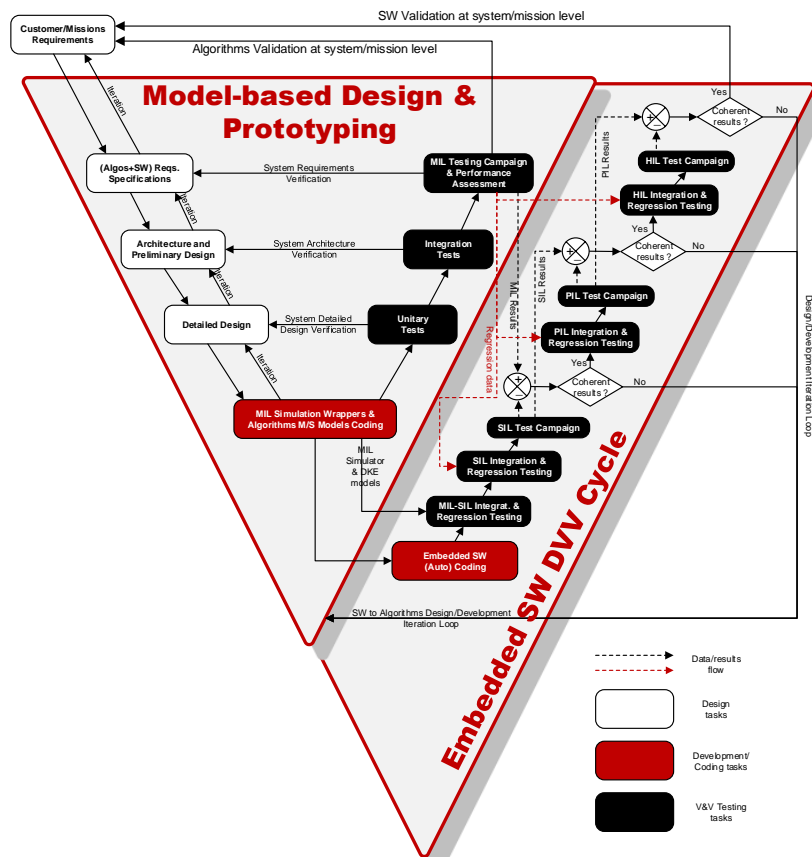


Fig. 3 AOCS/GNC SW lifecycle: Design, prototyping, SW development and validation.

The GNC/AOCS software life cycle is a structured and iterative process designed to ensure the development of reliable and efficient control systems for spacecraft. The diagram in Fig. 3 illustrates the entire chain composed of several key phases: design, prototyping, software development, and validation, each contributing critically to the system's overall performance and robustness.

The life cycle commences with the design phase, where mission objectives and system requirements are meticulously defined. Detailed models of spacecraft dynamics, environmental factors, and control algorithms are created at this stage to lay the groundwork for the

system architecture. Accurate modeling is crucial as it informs all subsequent development stages, ensuring that the system can handle the operational demands of the mission. Following the design phase, prototyping involves the creation of preliminary versions of the software to test and validate the initial designs. This step uses simplified implementations of control algorithms and system components to identify potential issues as early as possible. Prototyping allows for iterative refinement, ensuring that the design is feasible and that any necessary adjustments are made before full-scale development. In this phase, the validated designs from the prototyping stage are developed into a full-scale implementation. This involves detailed coding (or auto-coding from models in a model-based software engineering process), integration of different system modules, and extensive testing. The focus is on achieving high precision, reliability, and efficiency, which are vital for the complex operations that spacecraft must perform.

The final phase corresponds to validation, which involves rigorous testing to ensure that the software meets the mission requirements and initial design specifications. Validation employs a combination of simulation environments and hardware-in-the-loop testing to replicate real-world conditions. This ensures that the software is capable of performing reliably in the dynamic and unpredictable environment of space.

The V cycle model is an essential framework in the development and validation of AOCS/GNC systems. The left side of the V represents the system decomposition and design phases, while the right side corresponds to integration and validation phases. At each level, from system requirements to detailed design, corresponding validation steps ensure that both individual components and the overall system meet the specified requirements. This iterative process enhances the system's robustness and reliability by allowing continuous refinement and validation.

Modeling is a fundamental aspect of the AOCS/GNC design and validation process. Accurate models of spacecraft dynamics, environmental interactions, and control algorithms are essential for predicting system behavior and identifying potential issues. Through modeling, engineers can simulate various mission scenarios, evaluate the performance of control strategies, and optimize system parameters before actual deployment. This reduces the risk of operational failures and improves the overall success rate of missions. Modeling, therefore, is the backbone of the AOCS/GNC lifecycle, ensuring the development of systems that can perform reliably in space. More recently, modeling is also taking a new role with the rise of digital twins Fuller et al. (2020) as tools for algorithm design, machine learning training, software validation, and even predictive maintenance or operational planning and scheduling.

## 1.2 In-Orbit Servicing and Assembly

In-Orbit Servicing (IOS), which encompasses the repair, refueling, maintenance, or removal of space structures while in orbit, has been a conceptual focus since at least the 1970s. This interest originated from the potential of large space structures and was first practically realized in 1973 with the servicing of the Skylab space station Tatsch et al. (2006).

Despite this early milestone, the current real-world implementations of assembly and repair functionalities are relatively limited. Notable examples include the Shuttle Remote Manipulator System (SRMS) and the Space Station Remote Manipulator System (SSRMS) aboard the International Space Station (ISS). These systems, however, are entirely teleoperated, either from onboard the spacecraft or from the ground, lacking any form of autonomy.

In a modern definition, servicing is defined as the on-orbit modification of a satellite or its orbit after its initial launch, performed by another spacecraft. This process includes tasks such as relocating the satellite to a new orbit, refueling, repairing broken parts, replacing components, deploying systems that failed to deploy post-launch, and cleaning various components Carioscia et al. (2018). There have been successful demonstrations of on-orbit assembly subsystems. For instance, the Robot Technology Experiment (ROTEX), a German experiment conducted by NASA, and the Engineering Test Satellite (ETS-VII), launched by the Japanese Aerospace Exploration Agency (JAXA), have shown the feasibility and potential of these technologies. These experiments represent significant steps towards more advanced and autonomous on-orbit servicing capabilities, indicating a promising future for the field. The interested reader is referred to the survey in Flores-Abad et al. (2014) for additional examples of demonstrations of potential IOS cases.

In a similar line, the aerospace industry has been researching and practicing In-Orbit Assembly (IOA) technology for decades. A significant milestone in this journey was in 1985 when the NASA and the ESA began collaborative studies on orbital assembly. This collaboration utilized the space shuttle to conduct the EASE/ACCESS experiments during the STS-61-B mission Li et al. (2022). These experiments involved constructing a truss structure on-orbit using manual assembly techniques at a workstation. This foundational work played a crucial role in the subsequent development of the International Space Station (ISS) program. The Autonomous Assembly of a Reconfigurable Space Telescope (AAReST) Underwood et al. (2015) demonstrated the technology needed for telescope elements to position and attach themselves on orbit. The system comprises mirror segments and a cluster of CubeSats that can undock and navigate autonomously.

The modern view on assembly involves the on-orbit aggregation of components to form a spacecraft into a new shape or configuration, particularly (though not exclusively) those that cannot be achieved through traditional deployment methods and current launch vehicles. The assembly process can be conducted by the spacecraft itself using a robotic arm, by a free-flying companion spacecraft launched alongside the satellite, or by a third-party spacecraft commissioned later for this task. These components can be either launched from the ground or manufactured in orbit Carioscia et al. (2018). Therefore, in terms of applications, it could prove useful for the construction of telescopes too large to be fully built on Earth and launched into orbit Roa Garzon et al. (2019); for weather and climate observations, it can mean a reduction of satellite launches by creating a persistent platform assembled in space; construction of large antennas Briz et al. (2023); Colmenarejo et al. (2018); or even provide significant advantages for commercial missions, particularly communication satellites in Geosynchronous Earth Orbit (GEO) Boyd et al. (2017). These applications and potential outcomes are illustrated in Fig. 4.

Both IOA and IOS have long been recognized as an efficient method for constructing and maintaining large space platforms, providing

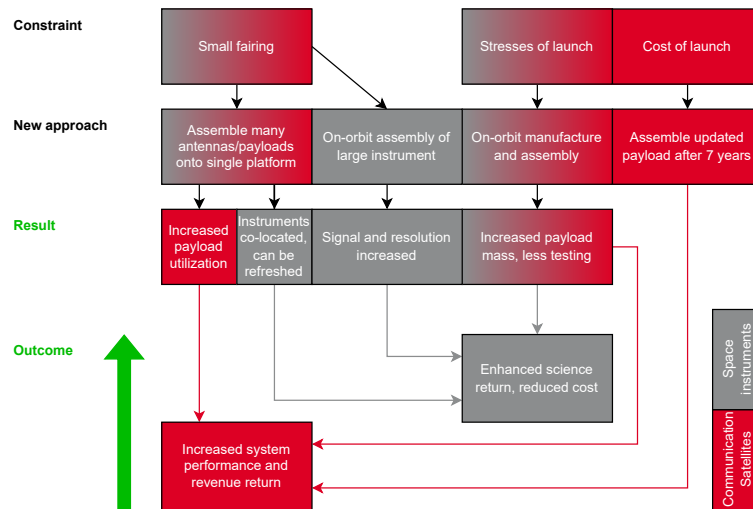


**Fig. 4** How on-orbit manufacturing and assembly approaches could alleviate limitations associated with current approach to deploying space instruments and communications satellites to enhance science return and system performance, reduce cost, and increase revenue return (adapted and reworked from Boyd et al. (2017))

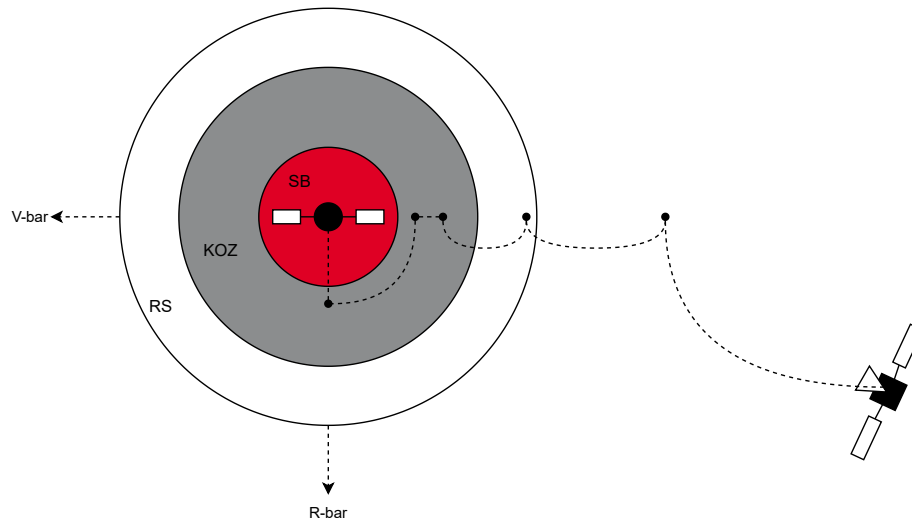


**Fig. 5** A typical rendezvous sequence along with the safety areas (keep-out zone, rendezvous sphere, safety boundary).

a versatile approach to building complex structures in space. This technology is crucial for supporting a range of significant projects, including manned moon landings, high-orbit space stations, solar power plants, and various other major national and international space initiatives Arney et al. (2021). The importance of on-orbit assembly extends beyond mere construction; it is fundamental to the advancement of the aerospace field. Space robots, integral to this technology, drive advancements in control technology, dynamics, redundant degree of freedom path planning, vision systems, and sensing technology. Furthermore, research into space station robots can foster interdisciplinary advancements in fields such as human factors engineering. Consequently, the deployment of space robots for on-orbit assembly not only accelerates the progress of aerospace projects but also stimulates breakthroughs in related technological domains, underscoring its dual significance in promoting both the development of space infrastructure and related technological innovations.

### 1.3 Challenges

A typical mission for a spacecraft can be split into the following phases as illustrated in Fig. 5:

- *Far-range* — characterized by orbit transfer and phasing, this segment of the mission is typically controlled from the ground station. The vehicle closes in either in autonomous or semi-autonomous based on coarse metrology.
- *Close-range* — the spacecraft is closer to the target and must fly-around it while synchronizing their relative motion before the close proximity.

- *Close proximity* — this is the most critical part where the spacecraft will either capture, dock, or berth, depending on the mission objective and the autonomy of the target vehicle. Various other steps can be included like cargo transfer, refueling, servicing, robotic manipulation, etc.
- *Aftermath* — it corresponds to the separation from the target until a safe distance is achieved and an orbit transfer to idle orbit

The far- and close-range (as well as aftermath, which is essentially a reversed close/far-range approach) present some interesting control challenges and are the phases where most commonalities between all types of proximity and formation flying missions can be found. In all these phases, there could be a set of challenges to be tackled, namely:

**Recurrence.** The advent of in-orbit servicing and assembly, as well as the future space logistics (based on an ecosystem of reusable vehicles - launchers, spaceplanes and re-entry vehicles, and space tugs / ferries) introduces the concept of recurrent flight. This means that a single vehicle is required to recover cargo, e.g. a stack of reflectors to assemble an antenna or telescope, from a parking orbit to the destination several times as the cargo is being launched by smaller launchers. Doing so introduces significant cost and operational constraints, in particular due to propellant consumption. Therefore, finding ways to perform the far-range approach (where most propellant is expended) more efficiently is paramount for the realization of these new applications.

**Adaptability.** Servicers and space tugs will be required to handle changes in the type of mission to perform (e.g. from the parking orbit to a new destination, from the destination to a refueling depot, etc.), changes in the mission conditions (added payload to/from the same parking orbit, for example), changes during the mission execution (failures, faults, any anomaly in the system or in the logistic ecosystem that requires delivery on a different port/orbit), or even changes to the vehicle (upgrading sensors, actuators, software). To achieve this, fault tolerant, adaptive, and modular control systems are necessary to be able to cope with uncertainties, disturbances, and faults, adapt to different missions and payloads, and integrate new components and software updates.

**Safety.** This, as adaptability, is a prevalent consideration in all the phases. However, the specific considerations are significantly different. Rendezvous is performed as a set of hops between safe hold points (HP) approaching the target vehicle through V-bar (the axis tangent to the orbit, collinear with the target velocity in circular orbits) or through R-bar (the radial axis of the orbit) as shown in figure 5. These hops are fly-arounds, drift orbits, straight-lines, transfers, among others. The concept of operations specifies keep-out zones (KOZ), rendezvous spheres (RS), and safety boundaries (SB) that have different impacts on each phase and that inform the selection of the HPs. While in close proximity one has to consider the necessary agility and precision (including collision avoidance) on the relative pose, at the far-range the main safety aspects lie on the trajectory design – the vehicle must acquire passively safe relative orbits with respect to the target. In the far-range, the RS is the outer safety layer typically of the order of tens of kilometers, outside of which the safety of each manoeuvre must be passively guaranteed. Passive safety is defined as a strategy that avoids collisions (or, in this case, entering the RS) even in the presence of possible thruster failures and malfunctions, i.e., a trajectory that without active control results in an orbit that does not enter the RS. Next, the KOZ is a smaller sphere (e.g. 1 km) that is only penetrated in the final, closer approach. Finally, the SB is a smaller sphere (around 100 m) based on the size of the two vehicles. This boundary can only be entered in a closed-loop controlled way to start the close proximity operations.

**Knowledge.** Given that controllers often rely on models in order to have assurances of performance and possibly robustness, knowledge of parameters, disturbance characteristics, and trajectories that maintain observability of the system from the available set of measurements are all pieces of information that are key for every phase.

**Robustness.** This is a natural product of adaptability and knowledge in the sense that the controller will be robust to different conditions if the designer can have a sufficiently good knowledge of the model and the control law is sufficiently able to adapt to each scenario. Typically, close range maneuvers are more problematic given the impact that a relative error has on the safety of the mission.

**Verification and Validation.** Through verification, we ensure that the system accurately implements the intended design, while validation confirms that the system meets the required operational needs under real-world conditions. This issue is fundamental in establishing trust on the methodologies and approaches, confirming the accuracy of the software and assess closed-loop properties like convergence, stability and performance guarantees.

Therefore, the issues affecting the different types of mission are different and divided by the aforementioned types. In the development of servicing technology, challenges were primarily due to the lack of cooperation, as most existing satellites were not designed to be serviced. In contrast, assembly issues were largely related to systems-level challenges, such as assembly procedures, optimization, and precision. Safety, certification, and validation processes are anticipated to be the main obstacles to assembling and manufacturing satellites in space. Many technologies will need to be demonstrated and perfected on smaller missions before being employed in flagship or human-rated missions. Examples of these precursor technologies include relative navigation systems, robotics, refueling, and avionics. The processes for servicing an active satellite versus servicing a disabled or inactive object (which might be unstable or tumbling) are different. Tumbling and uncontrollable satellites require greater maneuverability from a servicer during the capture phase than if the client were three-axis stable.

## 2 Moving in Space

The motion of spacecraft in orbit is governed by a set of phenomena (gravity, atmospheric drag, solar radiation pressure, etc.) that can be categorized as:

1. **Orbital mechanics**, which model the translational motion of the spacecraft with respect to the body(ies) that it is orbiting driven by

gravitational (primary and third bodies) and tidal forces. These are obviously nonlinear, even in their simplest form which considers Keplerian motion, i.e., a point mass orbiting a spherical central body.

2. **Attitude kinematics and dynamics**, usually seen as rigid body dynamics.
3. **Disturbances**, including internal phenomena such as propellant sloshing (see Dodge (2000)) or flexible appendages (see Alazard et al. (2008)), and external stimuli like solar radiation pressure, atmospheric drag, gravity gradient, magnetic torques.
4. **Actuators**, which include systems capable only of exerting torques such as momentum exchange (reaction wheels, control momentum gyroscopes) and magnetic equipment (magnetorquers), and propulsive devices such as chemical, cold gas, or electric thrusters (see Brown (1996a)). These actuators have very specific constraints: all have limitations in terms of maximum control authority, naturally, but thrusters are limited as well in their minimum opening times - the so called minimum impulse bit. Flywheels have also limitations on their angular momenta (and not only on the achievable torque) and present significant nonlinearities near zero rotation speed. All these present constraints on the control systems that can be neglected in the guidance and control designs in most situations but become more and more relevant with increased criticality, autonomy, and the necessity for efficiency and robustness.
5. **Contact dynamics**, when in very close proximity and during any physical interaction between two spacecraft Colmenarejo et al. (2018). This is important during capture, servicing, or any robotic operations in space.

Accurate and usable models for these dynamics elements are extensively available in the literature, for example in classic spacecraft dynamics, mission engineering, and GNC books such as Sidi (1997); Wie (2008); Wertz et al. (2011) or more recent references such as Yang (2019); Pesce et al. (2022).

## 2.1 Translational Motion

The typical IOS/IOA scenario orbiting the Earth involves at least two spacecraft in some form of proximity operations. For that reason, it is important to define the relative dynamics. Consider a chaser spacecraft, denoted as C, with a mass  $m_C$  and a target spacecraft T with mass  $m_T$  and at an altitude  $R_T$ . For the simplest model, the Earth is assumed to be a perfect sphere, with mass  $M_E$  and radius  $R_E$ . The universal gravitational constant is denoted by  $G$ , and the gravitational parameter of the Earth is  $\mu = GM_E$ . Note that the radius of the orbit of the target is then given by  $R_T + R_E$ .

To describe the dynamics of a spacecraft, we express the equations of motion (Newton's second law) within an inertial frame centered on, but not fixed to, the Earth. This inertial frame is also beneficial for tasks such as analyzing results. Assuming the spacecraft's masses are negligible compared to Earth's, their gravitational forces are disregarded. Additionally, the differences in accelerations due to the Sun's gravity are considered insignificant, and the gravitational influences of the Moon and other celestial bodies are neglected. Under these assumptions, the appropriate frame is the Earth-Centered Inertial (ECI) frame, which is defined with its origin at the Earth's center and is non-rotating. In this frame, the  $z$ -axis points to the North Pole, the  $x$ -axis points to the Earth's vernal equinox, and the  $y$ -axis completes a right-handed coordinate system.

For the control problem of managing the relative position of a chaser spacecraft with respect to a target spacecraft, a reference frame centered on the target is useful for the controller, as the target remains stationary in this frame, simplifying the dynamics. This reference frame is known as the Local Vertical Local Horizontal (LVLH) frame. The LVLH frame's origin is at the center of the target spacecraft, with the axes defined as follows: the  $z$  axis (also called  $R$ -bar) points from the target to the Earth's center; the  $y$ -axis is perpendicular to the orbital plane, pointing opposite to the target's angular momentum; and the  $x$  axis (also called  $V$ -bar) is tangent to the target's orbit, pointing in the direction of the target's velocity for circular orbits, forming a right-handed coordinate system. Figure 6 illustrates both frames and some variables used in transformations between them.

Let  $\mathbf{r}(t) = [x(t), y(t), z(t)]^T$  be the position of the chaser in the LVLH frame and  $\mathbf{r}_T(t)$  the position of the target (by definition equal to the center of the LVLH frame), then the position of the chaser in the ECI frame is given by

$$\mathbf{r}_{\text{ECI}}(t) = \mathbf{R}(t)\mathbf{r}(t) + \mathbf{r}_T(t), \quad (1)$$

where  $\mathbf{r}_{\text{ECI}}(t) = [x_{\text{ECI}}(t), y_{\text{ECI}}(t), z_{\text{ECI}}(t)]^T$  and  $\mathbf{R}(t)$  is the rotation matrix that transforms vectors from the LVLH frame to ECI frame, and that depends on the target's position in the orbit, as well as the orbit itself (in particular its eccentricity and inclination). The sequel will address the dynamics of  $\mathbf{r}_{\text{ECI}}(t)$  and  $\mathbf{r}_T(t)$ .

### 2.1.1 Orbital Dynamics

In the ECI frame, the dynamics of any celestial object S according to Newton's Second Law are given by

$$m_S \ddot{\mathbf{r}}_S(t) = m_S \ddot{\mathbf{r}}_{S_g}(t) + \mathbf{u}_S(t), \quad (2)$$

where dot notation represents the derivative with respect to time,  $\mathbf{u}_S(t)$  represents the forces applied on S, e.g. a control input for a spacecraft, and  $\ddot{\mathbf{r}}_{S_g}(t)$  is the acceleration due to gravity, itself given by Newton's Law of Universal Gravitation as

$$\ddot{\mathbf{r}}_{S_g}(t) = -\frac{\mu}{\|\mathbf{r}_S(t)\|^3} \mathbf{r}_S(t). \quad (3)$$

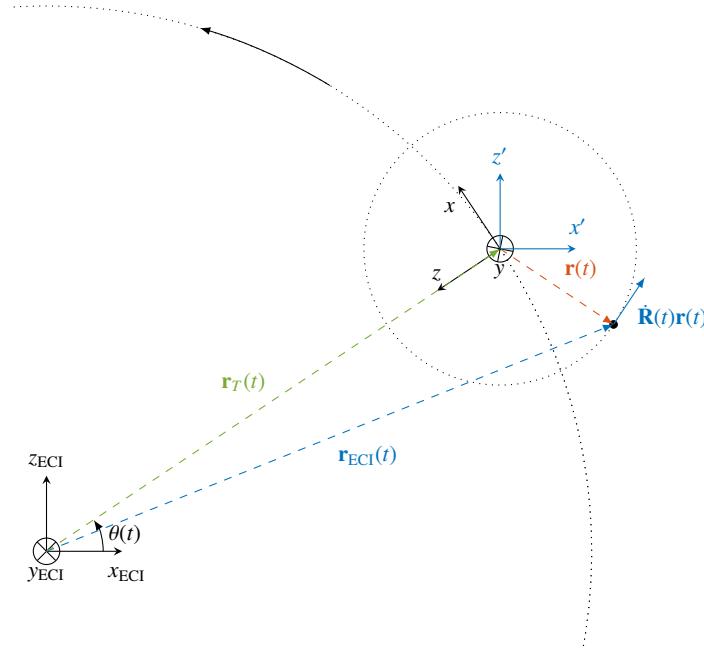


**Fig. 6** Relative motion of the chaser with respect to the target. Position of the chaser relative to the LVLH frame  $r(t)$  and relative to the ECI frame  $r_{\text{ECI}}(t)$ . LVLH frame rotated by  $\theta(t)$  (blue axes  $x'$  and  $z'$ ). Physical interpretation of  $\mathbf{R}(\theta(t))\mathbf{r}(t)$  (blue). Position of the target relative to the ECI frame  $r_T(t)$  (green).

Not considering external control forces, all acting forces are central-forces. Therefore, there is conservation of orbital angular momentum of the object. Hence, the orbital motion is planar and it is the same as Kepler's second law, which states that the swept out area during constant time intervals is constant. The solution is then a conic curve: Keplerian orbits are circular, elliptical, parabolic, or hyperbolic. For Earth-orbiting satellites, the first two categories are the most relevant. Assuming, circular orbits, the motion of a celestial object (with  $\mathbf{u}_S(t) = 0$ ) can be described as a circle, with its position entirely defined by the true anomaly angle  $\theta(t)$  and the orbital plane (see Figure 6).

### 2.1.2 Relative Dynamics

Considering our scenario of a chaser approaching a non-actuating target spacecraft, it is possible to write the relative dynamics as

$$\ddot{\mathbf{r}}_T(t) - \ddot{\mathbf{r}}_C(t) = \ddot{\mathbf{r}}_{T_g}(t) - \ddot{\mathbf{r}}_{C_g}(t) - \frac{1}{m_C}\mathbf{u}_C(t), \quad (4)$$

where the control input  $\mathbf{u}_C(t)$  will be described in Section 3.1.2. As described above, it is important to obtain the equations of motion in the LVLH frame, as the relative dynamics can be further simplified. First of all, recall (??), and take its first derivative

$$\dot{\mathbf{r}}(t) = \dot{\mathbf{R}}^\top(t)(\mathbf{r}_C(t) - \mathbf{r}_T(t)) + \mathbf{R}^\top(t)(\dot{\mathbf{r}}_C(t) - \dot{\mathbf{r}}_T(t)), \quad (5)$$

which, calling the last parcel  $\mathbf{v}(t)$  and noting that the derivative of  $\mathbf{R}\mathbf{a}$  is  $\mathbf{R}\boldsymbol{\omega} \times \mathbf{a}$ , with  $\boldsymbol{\omega}$  being the angular velocity of the LVLH frame with respect to the ECI frame, can be rewritten as

$$\dot{\mathbf{r}}(t) = -\boldsymbol{\omega} \times \mathbf{r}(t) + \mathbf{v}(t). \quad (6)$$

Taking now the derivative of  $\mathbf{v}(t)$  and following similar steps as above yields

$$\dot{\mathbf{v}}(t) = -\boldsymbol{\omega} \times \mathbf{v}(t) + \mathbf{R}^\top(t)(\ddot{\mathbf{r}}_C(t) - \ddot{\mathbf{r}}_T(t)). \quad (7)$$

Recalling (4) and replacing it in the above expression, allows to write

$$\dot{\mathbf{v}}(t) = -\boldsymbol{\omega} \times \mathbf{v}(t) - \frac{\mu}{\|\mathbf{r}_T(t)\|^3}\mathbf{R}^\top(t)\mathbf{r}_T(t) + \frac{\mu}{\|\mathbf{r}_T(t) + \mathbf{R}(t)\mathbf{r}(t)\|^3}\mathbf{R}^\top(t)(\mathbf{r}_T(t) + \mathbf{R}(t)\mathbf{r}(t)) - \frac{1}{m_C}\mathbf{R}^\top(t)\mathbf{u}_C(t), \quad (8)$$

where the chaser position is replaced using (1). Since this is a nonlinear expression, it is difficult to remove the explicit influence of the target position. However, these equations of relative motion in the LVLH frame can be simplified noting that the distance between the two spacecraft is much smaller than the orbital radius of either spacecraft, i.e.,  $\|\mathbf{R}(t)\mathbf{r}(t)\| \ll \|\mathbf{r}_T(t)\|$ . This is the basic assumption behind the model derived in the 60s by Clohessy and Wiltshire Clohessy and Wiltshire (1960), which will be further once we focus on the rendezvous

problem. The next step is then to simplify the above expression as follows

$$\dot{\mathbf{v}}(t) \approx -\boldsymbol{\omega} \times \mathbf{v}(t) - \frac{\mu}{\|\mathbf{r}_T(t)\|^3} \mathbf{R}^\top(t) \mathbf{r}_T(t) + \frac{\mu}{\|\mathbf{r}_T(t)\|^3} \mathbf{R}^\top(t) (\mathbf{r}_T(t) + \mathbf{R}(t) \mathbf{r}(t)) - \frac{1}{m_C} \mathbf{R}^\top(t) \mathbf{u}_C(t) \quad (9)$$

$$= -\boldsymbol{\omega} \times \mathbf{v}(t) + \frac{\mu}{\|\mathbf{r}_T(t)\|^3} \mathbf{r}(t) - \frac{1}{m_C} \mathbf{R}^\top(t) \mathbf{u}_C(t). \quad (10)$$

If the target is in a circular orbit, these can be further simplified resulting in the Clohessy-Wiltshire (CW) equations. This is the most common model for the far-range operations, where the timescale separation between translational and rotational motion is evident - allowing a complete decoupling of motion.

### 3 The Far-Range: Orbit Transfers and Rendezvous

Recall Section 1.3, where the phases of a IOS/IOA mission are described. The far-range is composed of the rendezvous between a chaser spacecraft and its target, including the orbit transfer, phasing, and the closing. In this phase, the distances involved are from hundreds of kilometers to hundreds of meters. Traversing such large distances safely takes a long time and is costly in terms of propellant and operations. The typical GNC architecture decouples translational and rotational motion - the former is handled by the guidance function (and actuation management) while the latter is left to the AOCS subsystem and is motivated by pointing to the target to extract relative measurements.

#### 3.1 Design models

The fact that the relative distance is quite large, it means that the attitude correction can often be ignored and dealt separately from the controller in charge of performing the rendezvous operation. In those cases, various simplifications have been used which we detail in the next subsections.

##### 3.1.1 The Clohessy-Wiltshire Equations

For the controller, it is useful to describe the dynamics of the spacecraft through a set of equations that are simpler than the full dynamics. The Clohessy-Wiltshire (CW) equations Clohessy and Wiltshire (1960) describe the relative motion of a spacecraft in orbit around a central body. The equations are derived by linearizing the full dynamics around a circular orbit. The equations, in the LVLH frame centered on the target are given by

$$\begin{cases} \ddot{x}(t) - 2\omega\dot{z}(t) &= \frac{F_x(t)}{m_c} \\ \ddot{y}(t) + \omega^2 y(t) &= \frac{F_y(t)}{m_c} \\ \ddot{z}(t) + 2\omega\dot{x}(t) - 3\omega^2 z &= \frac{F_z(t)}{m_c} \end{cases}, \quad (11)$$

where  $\omega$  is the angular velocity of the target around the Earth,  $m_c$  is the mass of the chaser, and  $\mathbf{F}(t) = [F_x(t), F_y(t), F_z(t)]^\top$  is the force applied to the chaser. (11) can be rewritten in a linear state-space form

$$\dot{\mathbf{x}}(t) = \mathbf{A}_c \mathbf{x}(t) + \mathbf{B}_c \mathbf{u}(t), \quad (12)$$

where

$$\mathbf{x}(t) = \begin{bmatrix} x(t) \\ y(t) \\ z(t) \\ \dot{x}(t) \\ \dot{y}(t) \\ \dot{z}(t) \end{bmatrix}, \quad \mathbf{u}(t) = \begin{bmatrix} F_x(t) \\ F_y(t) \\ F_z(t) \end{bmatrix}, \quad \mathbf{A}_c = \begin{bmatrix} 0 & 0 & 0 & 1 & 0 & 0 \\ 0 & 0 & 0 & 0 & 1 & 0 \\ 0 & 0 & 0 & 0 & 0 & 1 \\ 0 & 0 & 0 & 0 & 0 & 2\omega \\ 0 & -\omega^2 & 0 & 0 & 0 & 0 \\ 0 & 0 & 3\omega^2 & -2\omega & 0 & 0 \end{bmatrix}, \quad \mathbf{B}_c = \begin{bmatrix} 0 & 0 & 0 \\ 0 & 0 & 0 \\ 0 & 0 & 0 \\ \frac{1}{m_c} & 0 & 0 \\ 0 & \frac{1}{m_c} & 0 \\ 0 & 0 & \frac{1}{m_c} \end{bmatrix}. \quad (13)$$

##### 3.1.2 Actuation

Propulsion systems used in spacecraft vary in complexity and capabilities. Currently, many propulsion technologies are available Krejci and Lozano (2018). There are chemical and electric propulsion systems, with different types of thrusters. Within chemical propulsion, there are several types of thrusters, such as monopropellant, bipropellant, and cold gas thrusters. These thrusters all share the same principle of operation: a propellant is heated and expelled through a nozzle, generating thrust.

Ideally, a thruster would be able to instantly supply one hundred percent of its rated thrust for any amount of time, and instantly stop when commanded to do so. In reality, this is not the case. Thrusters have some response delay and a minimum amount of time they can be on for. Moreover, they take some time to reach their maximum thrust, and some time to stop. In this paper, we will consider a simplified model of a thruster, discarding the delay and rise and fall times, effectively applying a constant force in a single direction for a given amount of time. Figure 7 illustrates a typical thruster pulse, and a rectangular pulse approximation.

For a spacecraft with  $M$  actuators, assuming each actuator is allowed at most a single pulse, the control input  $\mathbf{u}$  is given by

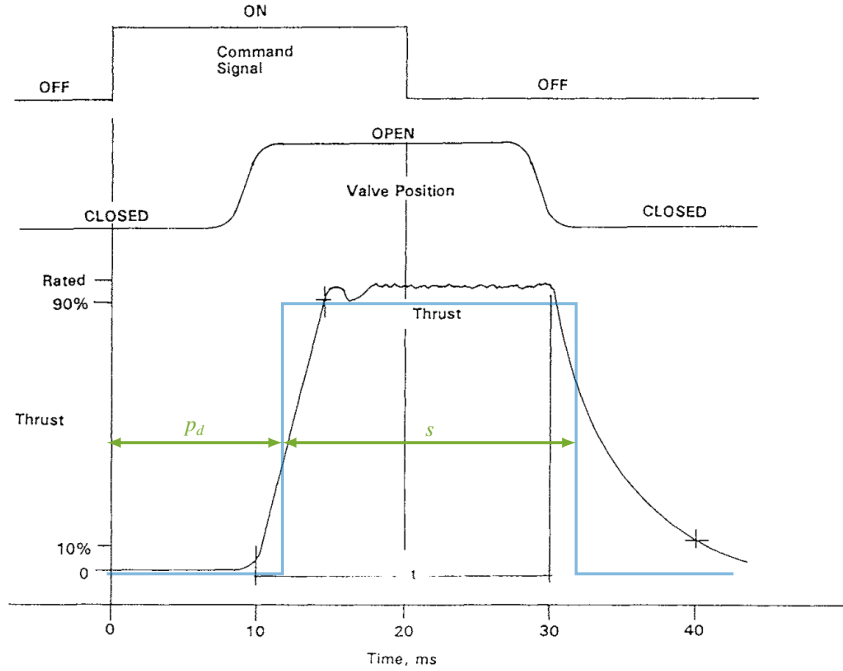


**Fig. 7** Realistic thruster pulse. The thruster takes some time to reach its maximum thrust, and some time to stop. Approximation of a thruster pulse with a rectangular pulse (blue). Pulse delay  $p_d$  and duration  $s$ . The delay is not considered. Adapted from Brown (1996b).

$$\mathbf{u}(t) = \sum_{i=1}^M F_i \mathbf{w}_i (H(t - \tau_i - s_i) - H(t - \tau_i)) \quad (14)$$

$$H(t) = \begin{cases} 1 & \text{if } t \geq 0 \\ 0 & \text{if } t \leq 0 \end{cases}, \quad (15)$$

where, for actuator  $i$ ,  $t_i^{\min} \in \mathbb{R}^+$  is its minimum pulse duration,  $F_i \in \mathbb{R}$  is the maximum magnitude of the force applied by itself,  $\mathbf{w}_i \in \mathbb{R}^3$  is a unit vector in the direction of the force, and  $H(t - \tau_i - s_i) - H(t - \tau_i)$  is a unit pulse denoting its state, which is 1 (on) starting at  $\tau_i \in \mathbb{R}$  for the duration  $s_i \in \mathbb{R}^+$ , and 0 (off) the rest of the time.

In general, several pulses may be applied, such that

$$\mathbf{u}(t) = \sum_{i=1}^M F_i \mathbf{w}_i \sum_{p=1}^P H(t - \tau_i^p - s_i^p) - H(t - \tau_i^p), \quad (16)$$

where each actuator is turned on at most  $P$  times, with the  $p^{\text{th}}$  pulse for actuator  $i$  starting at  $\tau_i^p$  and lasting for  $s_i^p$ .

It is also necessary to ensure that the pulses do not overlap, which can be done by ensuring that the start of the next pulse occurs after the end of the previous pulse, and the minimum pulse duration is respected, i.e.

$$\tau_i^{p+1} \geq \tau_i^p + s_i^p + t_i^{\min}. \quad (17)$$

### 3.1.3 Discretizing the Dynamics

In the notation used for discrete time, the time variable is represented as an index  $k$ , representing the time at  $t = kT$  (e.g.  $x_k$  represents  $x(kT)$ ).

The discrete dynamics can be obtained from the continuous dynamics as

$$\mathbf{x}_{k+1} = e^{\mathbf{A}_c T} \mathbf{x}_k + \sum_{i=1}^M \int_0^T e^{\mathbf{A}_c(T-\tau)} \mathbf{B}_c \mathbf{u}_i(\tau) d\tau, \quad (18)$$

where  $T \in \mathbb{R}^+$  is the sampling time, and  $e^{\mathbf{A}_c t}$  is the matrix exponential of  $\mathbf{A}_c$ , given by

$$e^{\mathbf{A}_c t} = \begin{bmatrix} 1 & 0 & 6(\omega t - \sin(\omega t)) & \frac{4}{\omega} \sin(\omega t) - 3t & 0 & \frac{2}{\omega}(1 - \cos(\omega t)) \\ 0 & \cos(\omega t) & 0 & 0 & \frac{1}{\omega} \sin(\omega t) & 0 \\ 0 & 0 & 4 - 3 \cos(\omega t) & \frac{2}{\omega}(\cos(\omega t) - 1) & 0 & \frac{1}{\omega} \sin(\omega t) \\ 0 & 0 & 6\omega(1 - \cos(\omega t)) & 4 \cos(\omega t) - 3 & 0 & 2 \sin(\omega t) \\ 0 & -\omega \sin(\omega t) & 0 & 0 & \cos(\omega t) & 0 \\ 0 & 0 & 3\omega \sin(\omega t) & -2 \sin(\omega t) & 0 & \cos(\omega t) \end{bmatrix}. \quad (19)$$

For actuator  $i$ , assuming the control input is applied at the beginning of each time step (applied for  $s_i \in [0, T)$ ), we can calculate the input part of the dynamics as

$$\int_0^T e^{\mathbf{A}_c(T-\tau)} \mathbf{B}_c \mathbf{u}_i(\tau) d\tau = e^{\mathbf{A}_c T} \int_0^{s_i} e^{-\mathbf{A}_c \tau} \mathbf{B}_c F_i \mathbf{w}_i d\tau \quad (20)$$

$$= e^{\mathbf{A}_c T} \int_0^{s_i} e^{-\mathbf{A}_c \tau} d\tau \mathbf{B}_c F_i \mathbf{w}_i \quad (21)$$

$$= e^{\mathbf{A}_c T} \mathbf{G}(s_i) \mathbf{B}_c F_i \mathbf{w}_i, \quad (22)$$

where

$$\mathbf{G}(s) = \int_0^s e^{-\mathbf{A}_c \tau} d\tau = \begin{bmatrix} s & 0 & -3s^2\omega + \frac{6(1-\cos(\omega s))}{\omega} & \frac{3s^2}{2} + \frac{4(\cos(\omega s)-1)}{\omega^2} & 0 & \frac{2s}{\omega} - \frac{2\sin(\omega s)}{\omega^2} \\ 0 & \frac{\sin(\omega s)}{\omega} & 0 & 0 & \frac{\cos(\omega s)-1}{\omega^2} & 0 \\ 0 & 0 & 4s - \frac{3\sin(\omega s)}{\omega} & \frac{2\sin(\omega s)}{\omega^2} - \frac{2s}{\omega} & 0 & \frac{\cos(\omega s)-1}{\omega^2} \\ 0 & 0 & 6\omega s - 6\sin(\omega s) & \frac{4\sin(\omega s)}{\omega} - 3s & 0 & 2\frac{\cos(\omega s)-1}{\omega} \\ 0 & 1 - \cos(\omega s) & 0 & 0 & \frac{\sin(\omega s)}{\omega} & 0 \\ 0 & 0 & 3(\cos(\omega s) - 1) & 2\frac{1-\cos(\omega s)}{\omega} & 0 & \frac{\sin(\omega s)}{\omega} \end{bmatrix}. \quad (23)$$

The matrix describing the dynamics of the actuator  $\mathbf{G}$  is a non-linear function of the time the actuator is on,  $s$ .  $e^{\mathbf{A}_c t}$  and  $\mathbf{G}(s)$  were computed using symbolic computation software.

The non-linear discrete-time dynamics are then given by

$$\mathbf{x}_{k+1} = \mathbf{A} \mathbf{x}_k + \mathbf{A} \sum_{i=1}^M \mathbf{G}(s_i) \mathbf{B}_c F_i \mathbf{w}_i, \quad (24)$$

where  $\mathbf{A}$  is the state transition matrix,  $\mathbf{A} = e^{\mathbf{A}_c T}$ .

### 3.1.4 Linearization of the Discrete Actuator Dynamics

The discrete actuator dynamics  $\mathbf{G}(s)$  are non-linear with respect to the control variables. It is beneficial to linearize the dynamics around a point  $s_0$ , so that also techniques from linear systems can be employed. That is

$$\mathbf{G}(s) \approx \mathbf{G}(s_0) + \left. \frac{\partial \mathbf{G}}{\partial s} \right|_{s=s_0} (s - s_0) := \tilde{\mathbf{G}}(s, s_0) \quad (25)$$

where  $\left. \frac{\partial \mathbf{G}}{\partial s} \right|_{s=s_0}$  is the element-wise derivative of  $\mathbf{G}(s)$  with respect to  $s$  evaluated at  $s_0$ .

$$\left. \frac{\partial \mathbf{G}}{\partial s} \right|_{s=s_0} = \begin{bmatrix} 1 & 0 & 6s_0\omega - 6\sin(\omega s_0) & \frac{4}{\omega} \sin(\omega s_0) - 3s_0 & 0 & \frac{2}{\omega}(1 - \cos(\omega s_0)) \\ 0 & \cos(\omega s_0) & 0 & 0 & \frac{1}{\omega} \sin(\omega s_0) & 0 \\ 0 & 0 & 4 - 3 \cos(\omega s_0) & \frac{2}{\omega}(\cos(\omega s_0) - 1) & 0 & \frac{1}{\omega} \sin(\omega s_0) \\ 0 & 0 & 6\omega(1 - \cos(\omega s_0)) & 4 \cos(\omega s_0) - 3 & 0 & 2 \sin(\omega s_0) \\ 0 & -\omega \sin(\omega s_0) & 0 & 0 & \cos(\omega s_0) & 0 \\ 0 & 0 & 3\omega \sin(\omega s_0) & -2 \sin(\omega s_0) & 0 & \cos(\omega s_0) \end{bmatrix}. \quad (26)$$

Note that

$$\tilde{\mathbf{G}}(s, 0) = \mathbf{0}_{6 \times 6} + s \mathbf{I}_{6 \times 6} = s \mathbf{I}_{6 \times 6}, \quad (27)$$

which is equivalent to fully disregarding the actuator dynamics over the pulse duration, and directly applying force proportional to the pulse

duration at the beginning of the pulse.

To demonstrate this, it is only necessary to recalculate the discrete dynamics calculation from (18), but instead of  $\mathbf{u}_i$ , we use  $\bar{\mathbf{u}}_i(\tau) = \delta(\tau) s_i F_i \mathbf{w}_i$ , where  $\delta(\tau)$  is the Dirac delta function. Indeed,

$$\int_0^T e^{\mathbf{A}_c(T-\tau)} \mathbf{B}_c \bar{\mathbf{u}}_i(\tau) d\tau = e^{\mathbf{A}_c T} \int_0^T e^{\mathbf{A}_c \tau} \delta(\tau) d\tau \mathbf{B}_c s_i F_i \mathbf{w}_i \quad (28)$$

$$= e^{\mathbf{A}_c T} \mathbf{B}_c s_i F_i \mathbf{w}_i \quad (29)$$

$$= e^{\mathbf{A}_c T} (\mathbf{0}_{6 \times 6} + s \mathbf{I}_{6 \times 6}) \mathbf{B}_c F_i \mathbf{w}_i \quad (30)$$

$$= e^{\mathbf{A}_c T} \bar{\mathbf{G}}(s, 0) \mathbf{B}_c F_i \mathbf{w}_i. \quad (31)$$

### 3.2 Literature

Given the simplifications to a linearized version of the dynamics, the task of performing rendezvous operations can benefit from the large body of knowledge related to linear systems. For instance, the work in Carter and Briant (1992) specified an optimal control problem subject to the linear dynamics that is equivalent to the Linear Quadratic Regulator (LQR) problem. This means that the optimal control action with respect to fuel consumption can be calculated from evaluating the state and costate dynamics that are typical in the LQR type of solutions. The same type of problem has been investigated in Chen and Fujimoto (2018) with the analytic solutions corresponding to the Hamilton-Jacobi-Bellman (HJB) equations for the problem.

The optimal solution for the optimal fuel problem is traditionally referred to as the primer vector theory. In Koenig and D'Amico (2021), the authors identified different cost functions depending on the spacecraft configuration. For instance,  $\|\mathbf{u}\|_2$  is used when the spacecraft can align a single thruster with the desired maneuver direction whereas  $\|\mathbf{u}\|_1$  corresponds to instances where the spacecraft has fixed attitude and three pairs of thrusters mounted on opposite sides on mutually perpendicular axes. A combination of  $\ell_2$  and  $\ell_1$  norms can be employed if there is a mixture between fixed axis thrusters and pairs that are mounted perpendicularly. The authors of Koenig and D'Amico (2021) then reformulate the fuel optimal problem as that of finding a minimizing cost such that the target state is contained in the reachable set of the chaser.

The literature also includes linear controllers based on inverting the linearized Clohessy-Wiltshire (CW) equations like the work in Lizy-Destrez et al. (2017). The authors propose a linear targeting controller that directs the velocity vector to point to the desired position. Nonlinear dynamics can be used with a shooting method to then correct the linear controller based on the error of the vehicle with respect to that estimated by the CW equations.

At great distances from the target, ground information is used for the navigation and trajectory planning. After detection of the target with the on-board sensors (narrow angle cameras), there is still some uncertainty on the relative position as the target's image starts sub-pixel and depth information is only available in much closer distances. This raises the need for bearings-only navigation and introduces significant uncertainties, against which the guidance and control functions must be very robust. A possible approach to reduce this uncertainty given in Serra et al. (2021) is to introduce navigation performance considerations in the trajectory design, i.e., to design or optimize spacecraft trajectories that improve observability of the target and reduce navigation uncertainty.

### 3.3 Challenges and Further Work

As we have discussed in this section, far-range maneuvers in spacecraft operations pose several key challenges that must be addressed to ensure mission success. One of the primary challenges is the accurate modeling and prediction of orbital dynamics over extended periods, which is complicated by gravitational perturbations from celestial bodies, atmospheric drag, and other environmental factors. Precise relative navigation between spacecraft, crucial for rendezvous and docking missions, is hampered by sensor limitations and the inherent uncertainties in state estimation. Additionally, communication delays and constraints can impact the timely execution of maneuvers, necessitating robust autonomous systems capable of making real-time decisions. Fuel efficiency is another critical concern, as far-range maneuvers often require substantial propellant usage, thus optimization of thrust vectors and maneuver planning is essential to conserve resources. These challenges point to the need of controllers that can incorporate a level of optimization in the produced actuation signals.

The challenges for far-range rendezvous maneuvers of spacecraft can be grouped as:

**Recurrence** — future reusable vehicles and the objectives of servicing and assembly missions introduce the concept of recurrent flight.

Consequently, recurrence imposes strict constraints on fuel consumption, especially since far-range maneuvers are where the majority of the propellant is expended.

**Adaptability** — given the potential for varying mission conditions, anomalies, and upgrades during operation, it is essential to design fault-tolerant, adaptive, and modular control systems capable of managing uncertainties, disturbances, and faults.

**Safety** — ensuring safety during far-range rendezvous requires accurate trajectory design to prevent collisions and maintain passive safety, ensuring that trajectories remain safe even in the event of thruster failures.

**Robustness** — addressing recurrence and propellant efficiency requires precise system modeling for trajectory optimization to avoid corrections due to unmodelled dynamics. Therefore, incorporating factors such as orbital perturbations (solar radiation pressure, atmospheric drag, non-spherical gravity terms) and the finite duration of maneuvers into the design results in strategies that better tackle the above challenges.

**Verification** — complex algorithms for long distance motion that might require iterative computations on-board raise significant issues both in terms of their validation in the closed loop (stability, convergence, etc.) but also in ensuring reliable and repeatable real-time operation of the software.

Accommodating recurrent missions and the stringent safety standards results in the space industry adopting conservative approaches, favoring the use of well-established tools and theoretical methods that prioritize safety, robustness, and reliability over cutting-edge performance. Consequently, solutions often rely on open-loop control systems, where errors are allowed to accumulate and are only corrected during scheduled maneuver adjustments Fehse (2003). Additionally, thrust allocation is typically managed by a separate unit responsible for determining the firing intervals for the thrusters Bezerra and Santos (2021); Ankersen et al. (2005).

A recent proposal to tackle the rendezvous phase is to resort to Model Predictive Control (MPC), which can encompass discrete actuation states (e.g., on or off) through the use of binary variables for these states and employing a Mixed Integer Programming (MIP) solver. MIP optimization problems include both discrete and continuous variables and are typically solved using algorithms such as the branch-and-bound algorithm, widely implemented by solvers like Gurobi Gurobi Optimization, LLC (2022). However, these algorithms are not suitable for real-time applications due to their worst-case exponential complexity, which results from the extensive search required to find feasible solutions.

The work in Malyuta and Açikmeşe (2020) proposes a one-shot convex optimization method designed to achieve globally optimal solutions for a specific class of MIP non-convex optimal control problems caused by the incorporation of the minimum opening constraint of thrusts. The authors transform the non-convex formulation into a convex problem through a technique known as lossless convexification. They then prove that the optimal solution of the relaxed problem is almost always optimal for the original non-convex version. Utilizing second-order cone programming, the paper demonstrates that a significant class of optimal control problems with binary variables can be solved both reliably and in polynomial time.

In a similar direction, Tabora et al. (2024) proposes an MPC controller for spacecraft rendezvous that focus on the orbital control instead of the attitude component for far-range approaches which can be found in detail in Yang (2018). In this work, the computational complexity associated with the MIP arising from actuators constraints (e.g., thruster deadband due to minimum impulse bit (Brown, 1996a, Chapter 3)) by introducing an algorithm that iteratively fixes some of the actuations based on the solution of unconstrained versions of the optimization.

## 4 The Close-Range: Rendezvous and Proximity

The close-range segment of a rendezvous operation requires the spacecraft model to explicitly consider the attitude of the vehicle as well as stringent constraints to enforce safety. Apart from the full dynamics using rotation matrices, there has also been proposed the use of quaternions in the literature with the objective of having convex constraints to represent some of the typical conic restrictions for the attitude. In the next subsection, we introduce the constrained attitude problem and then make an overview of the literature related to this problem. In order to prepare the following part about further work that has been proposed for spacecraft but that it is yet to be standard in the industry, we will also cover the topic of Control Barrier Functions (CBFs).

### 4.1 Design models

The attitude control at the last stage of the rendezvous maneuver corresponds to change the orientation of the spacecraft from its current attitude given by the quaternion  $\mathbf{q}_0 \in \mathcal{S}^3$  to a final attitude corresponding to the quaternion  $\mathbf{q}_f \in \mathcal{S}^3$ . The trajectory of the attitude,  $\mathbf{q} : \mathbb{R}_0^+ \rightarrow \mathcal{S}^3$ , has boundary conditions  $\mathbf{q}(0) = \mathbf{q}_0$  and  $\mathbf{q}(t_f) = \mathbf{q}_f \otimes \varepsilon$ , where  $\varepsilon \in \mathcal{S}^3$  is some acceptable error. The trajectory must be such that a pointing vector  ${}^N\mathbf{v}(t) \in \mathcal{S}^2$  in the inertial reference frame  $\mathcal{N}$ , given by  ${}^N\mathbf{v}(t) = \mathbf{R}(\mathbf{q}(t)){}^B\mathbf{v}$  where  $\mathcal{B}$  is the body frame, at no point in time has an angle less than  $\theta_{out}$  with some pointing vector  ${}^N\mathbf{s} \in \mathcal{S}^2$ . Since  ${}^N\mathbf{v}$  and  ${}^N\mathbf{s}$  are both unit norm, this can be expressed as

$${}^N\mathbf{v} \cdot {}^N\mathbf{s} \leq \cos(\theta_{out}) \Leftrightarrow {}^N\mathbf{s}^\top(t)\mathbf{R}(\mathbf{q}(t)){}^B\mathbf{v}(t) \leq \cos(\theta_{out}), \forall t \in [0, \infty). \quad (32)$$

Likewise, we wish that a pointing vector  ${}^N\mathbf{d}(t) \in \mathcal{S}^2$  must at no point in time have an angle greater than  $\theta_{in}$  with another pointing vector  ${}^N\mathbf{e} \in \mathcal{S}^2$ , i.e.

$${}^N\mathbf{d} \cdot {}^N\mathbf{e} \geq \cos(\theta_{in}) \Leftrightarrow {}^N\mathbf{e}^\top(t)\mathbf{R}(\mathbf{q}(t)){}^B\mathbf{v}(t) \geq \cos(\theta_{in}), \forall t \in [0, \infty). \quad (33)$$

Therefore, at the final approach, the GNC subsystem must make the spacecraft converge to the target while at the same time ensuring safety by respecting constraints (32) and (33). The system state is composed of the attitude quaternion  $\mathbf{q}$  and the angular velocity in the body fixed frame  ${}^B\boldsymbol{\omega}$ , we thus get the state equation for our system that is given by

$$\dot{\mathbf{x}} = \begin{bmatrix} \dot{\mathbf{q}} \\ {}^B\dot{\boldsymbol{\omega}} \end{bmatrix} = \underbrace{\begin{bmatrix} -\frac{1}{2} \begin{bmatrix} -\mathbf{q}_v^\top \\ q_s \mathbf{I} + [\mathbf{q}_v]_\times \end{bmatrix} {}^B\boldsymbol{\omega} \\ {}^B\mathbf{J}^{-1}({}^B\mathbf{J}{}^B\boldsymbol{\omega} \times {}^B\boldsymbol{\omega}) \end{bmatrix}}_{\mathbf{f}(\mathbf{x})} + \underbrace{\begin{bmatrix} \mathbf{0} \\ {}^B\mathbf{J}^{-1} \end{bmatrix}}_{\mathbf{G}(\mathbf{x})} {}^B\boldsymbol{\tau}. \quad (34)$$

The vector  ${}^{\mathcal{B}}\boldsymbol{\tau}$  of coordinates of the total torque applied to the rigid body with respect to the body-fixed frame are the system's input. Given the limitations from the thrusters, there must be an imposed limit on the torque and angular velocity, as  $\|{}^{\mathcal{B}}\boldsymbol{\tau}\|_{\infty} \leq \tau_{max} = \max\{|{}^{\mathcal{B}}\tau_i| : i = 1, 2, 3\} \leq \tau_{max}$  and  $\|{}^{\mathcal{B}}\boldsymbol{\omega}\|_{\infty} \leq \omega_{max} = \max\{|{}^{\mathcal{B}}\omega_i| : i = 1, 2, 3\} \leq \omega_{max}$ , with  $\tau_{max}, \omega_{max} \in \mathbb{R}^+$ . Thus, the dynamics in (34) are control affine, meaning that they can be rewritten as

$$\dot{\mathbf{x}}(t) = \mathbf{f}(\mathbf{x}(t)) + \mathbf{G}(\mathbf{x}(t)){}^{\mathcal{B}}\boldsymbol{\tau}(t), \quad (35)$$

and the constrained attitude problem corresponds to the optimal control problem

$$\min_{{}^{\mathcal{B}}\boldsymbol{\tau}(t) \in \mathbb{R}^3, \mathbf{x} \in \mathbb{S}^3 \times \mathbb{R}^3} \Phi(\mathbf{x}(t_f)) + \int_0^{t_f} \|{}^{\mathcal{B}}\boldsymbol{\tau}(t)\|^2 dt \quad (36)$$

$$s.t. \quad \dot{\mathbf{x}}(t) = \mathbf{f}(\mathbf{x}(t)) + \mathbf{G}(\mathbf{x}(t)){}^{\mathcal{B}}\boldsymbol{\tau}(t) \quad t \in [0, t_f] \quad (37)$$

$$\mathbf{x}(0) = \mathbf{x}_0 \quad (38)$$

$${}^{\mathcal{N}}\mathbf{s}^{\top}(t)\mathbf{R}(\mathbf{q}(t)){}^{\mathcal{B}}\mathbf{v}(t) \leq \cos(\theta_{out}) \quad t \in [0, t_f] \quad (39)$$

$${}^{\mathcal{N}}\mathbf{e}^{\top}(t)\mathbf{R}(\mathbf{q}(t)){}^{\mathcal{B}}\mathbf{v}(t) \geq \cos(\theta_{in}) \quad t \in [0, t_f] \quad (40)$$

$$\|{}^{\mathcal{B}}\boldsymbol{\tau}(t)\|_{\infty} \leq \tau_{max} \quad t \in [0, t_f] \quad (41)$$

$$\|{}^{\mathcal{B}}\boldsymbol{\omega}(t)\|_{\infty} \leq \omega_{max} \quad t \in [0, t_f] \quad (42)$$

$$(43)$$

where  $\Phi(\mathbf{x}(t_f))$  is a terminal cost defined as  $\Phi(\mathbf{x}(t_f)) = \gamma \cdot (\max\{0, \mathbf{q}_f \cdot \mathbf{q}(t_f) - \varepsilon\})^2 + \eta \cdot \|{}^{\mathcal{B}}\boldsymbol{\omega}(t_f)\|^2$  with appropriate penalty weights  $\gamma \in \mathbb{R}^+$  and  $\eta \in \mathbb{R}^+$  and where  $\varepsilon$  is the cosine of the maximum angle we wish between the final quaternion  $\mathbf{q}(t_f)$  and target quaternion  $\mathbf{q}_f$ .

#### 4.1.1 Control Lyapunov Functions and Control Barrier Functions

Based on Lyapunov theory, there has been a recent interest from the community to use the concepts of Control Lyapunov Function (CLF) and CBF to design controllers that are both asymptotically stable and safe with respect to constraints like the ones in (32) and (33). The definition of a CLF is given as:

**Definition 1** (CLF Reis et al. (2021)). A positive definite function  $V : \mathbb{R}^n \rightarrow \mathbb{R}$  is said to be a CLF if, for the system described in equation (35) it satisfies

$$\inf_{\mathbf{u} \in \mathcal{U}} \{L_{\mathbf{f}}V(\mathbf{x}) + L_{\mathbf{G}}V(\mathbf{x})\mathbf{u}\} \leq -\gamma(V(\mathbf{x})), \quad \forall \mathbf{x} \in \mathcal{X}, \quad (44)$$

where  $\gamma : \mathbb{R}_0^+ \rightarrow \mathbb{R}_0^+$  is a class  $\mathcal{K}_{\infty}$  function.

Definition 1 is equivalent to saying that

$$K_{CLF}(\mathbf{x}) = \{\mathbf{u} \in \mathcal{U} : L_{\mathbf{f}}V(\mathbf{x}) + L_{\mathbf{G}}V(\mathbf{x})\mathbf{u} \leq -\gamma(V(\mathbf{x}))\} \neq \emptyset, \quad \forall \mathbf{x} \in \mathcal{X}, \quad (45)$$

i.e. we can create a feedback control law  $\mathbf{u} = \mathbf{k}(\mathbf{x})$  where,  $\mathbf{k} : \mathbf{x} \in \mathcal{X} \mapsto \mathbf{u} \in K_{CLF}(\mathbf{x})$ .

In a similar fashion, we can provide the definition of a CBF that maintains the system inside of a set  $C$  that is given as

$$C = \{\mathbf{x} \in \mathcal{X} : h(\mathbf{x}) \geq 0\} \quad (46)$$

as the following:

**Definition 2** (CBF Reis et al. (2021)). Let  $C$  be the set given by (46) where  $h$  is a continuously differentiable function. The function,  $h$ , is a control barrier function for system (35) if there exists an extended class  $\mathcal{K}_{\infty}$  function  $\alpha : \mathbb{R} \rightarrow \mathbb{R}$ , such that

$$\sup_{\mathbf{u} \in \mathcal{U}} \{L_{\mathbf{f}}h(\mathbf{x}) + L_{\mathbf{G}}h(\mathbf{x})\mathbf{u}\} \geq -\alpha(h(\mathbf{x})), \quad \forall \mathbf{x} \in C. \quad (47)$$

Like Definition 1, Definition 2 means that at every state  $\mathbf{x} \in \mathcal{X}$ , there exists a set of control inputs such that

$$K_{CBF}(\mathbf{x}) = \{\mathbf{u} \in \mathcal{U} : L_{\mathbf{f}}h(\mathbf{x}) + L_{\mathbf{G}}h(\mathbf{x})\mathbf{u} + \alpha(h(\mathbf{x})) \geq 0\} \neq \emptyset, \quad \forall \mathbf{x} \in C. \quad (48)$$

Thus, we can create a control law  $\mathbf{u}(t) = \mathbf{k}(\mathbf{x}(t))$  where  $\mathbf{k} : \mathbf{x} \in \mathcal{X} \mapsto \mathbf{u} \in K_{CBF}(\mathbf{x})$  that renders the safe set  $C$  positive invariant.

## 4.2 Literature

The typical approaches used by the industry are those that can be written in closed-form and then mathematically verified given the high-costs associated with a malfunction or an error in the trajectory. Under these tight constraints, Danielson et al. (2022) has proposed the use of robust positively invariant sets for the quaternion dynamics of the attitude to design a motion planner that can check for constraint satisfaction at a very fast rate (around 100,000 in less than 3 ms).

Another traditional approach is the use of potential functions with the idea that collisions can be defined as high values in the potential functions and then include the gradient of that function as to alter the velocity of the spacecraft towards values that are safe. An example has been introduced in Dong et al. (2017) where the authors define such a function that matches a sphere with the entry cone being with diminished cost. However, these strategies are not provably safe as can be obtained from the use of a CBF.

Safety has also been investigated by considering an ellipsoid around the spacecraft and requiring that the reachable sets always maintain a minimum  $\epsilon$  distance with any other ellipsoid. The authors in Guffanti and D'Amico (2022) has presented how to compute the ellipsoids and the control law to guarantee safety. These strategies are closely related to the robust positive invariant alternative in Danielson et al. (2022).

### 4.3 Challenges and Further Work

In the context of close-range rendezvous maneuvers, the nature of the challenges shifts significantly compared to far-range operations. Active safety becomes the main consideration, as the spacecraft must navigate within shorter distances to the target, often requiring precise control to avoid collisions. Propellant saving, while still a consideration, becomes less critical compared to the need for precise and agile maneuvers.

One of the primary challenges in close-range operations is the necessity to synchronize both the attitude and translational motion with the target, which may be tumbling or in an uncontrolled state. This synchronization is essential for safe docking, servicing, or assembly operations. Furthermore, an initial inspection phase is crucial when approaching from a safe orbit. During this phase, the spacecraft must assess the target to determine its mass, inertia properties, configuration, and any potential damage. This detailed inspection informs the planning and execution of subsequent phases, ensuring that the rendezvous and interaction with the target can be conducted safely and effectively.

The attitude synchronization maneuver involves transitioning the servicer from an initial position in the LVLH frame, where it maintains a target-pointing attitude, to a static position in the target body frame with an attitude defined relative to the target. Depending on the capture method, the servicer may need to precisely synchronize its motion with the target and maintain this synchronization while decreasing the relative distance.

The community has been focusing on the use of CBFs as an alternative to more traditional methods. For instance, in the paper Breeden and Panagou (2022) both landing and docking are defined in terms of forcing the derivative of the CBF  $h$  to be within an interval and reach zero at the final time for the maneuver. They then propose a Quadratic Program (QP) program that encompasses such a constraint, which from the theory of Lyapunov is a guaranteed to be safe.

In the literature subsection, we have identified that Danielson et al. (2022) and Guffanti and D'Amico (2022) have proposed techniques for spacecraft that ensures safety through the use of reachable sets. In that regard, the community can leverage recent advancements like the concept of Constrained Convex Generators (CCG) introduced in Silvestre (2022b). This set representation is capable of defining ellipsoids and polytopes and other combinations of sets. In particular, for dynamical models with uncertainties, it was shown in Silvestre (2022a) how to compute the convex hull of reachable sets to account for uncertainties while maintaining a polytopic descriptions. Later, Silvestre (2023) showed that in general CCG format, there exists a closed-form expression that is exact and avoids the exponential growth of the data structures in the set representation.

There has also been a lot of focus on MPC strategies for the guidance problem. These strategies are particularly enticing given their ability to easily encode constraints and their optimized control actions. The authors in Misra and Bai (2020) have proposed an MPC problem that encodes future feasibility of the MPC optimization to mitigate the main criticism of these strategies with respect to well established techniques. Namely, that if the problem is infeasible, it is problematic for the mission as the controller will not produce any action. The problem of rendezvous and docking has also been investigated using a MPC approach instead of a CLF-based QP (as in Breeden and Panagou (2022)) in the reference Weiss et al. (2015). Moreover, obstacle-avoidance can also be included in the MPC solutions using a single linear inequality constraint per state in the horizon as was presented in Silvestre and Ramos (2023).

## 5 In Close Proximity: The Highest Challenges

The phase of close proximity can include different objectives depending on the mission and degree of autonomy of the target vehicle. These can range from capture, docking or berthing and can include execution of cargo transfer, refueling, servicing, robotic manipulation, etc. A specific instance of interest is the Active Debris Removal (ADR) where recent efforts Branco et al. (2021) have increased the Technology Readiness Level (TRL) for such operations. The interested reader in ADR is directed to the review in Bonnal et al. (2013).

### 5.1 Literature and Challenges

In servicing scenarios, the target may be uncooperative and tumbling. A main difficulty is ensuring the rigidity of the structures composed of the servicer and the target that now should function as a single body. Different sets of problems can arise when the services is attempting to detumble, transfer fluid, de-orbit or robotic manipulation of the target. This segment is an active field of research with missions still in the design phase, which motivated a different organization of this section into a single subsection containing advances in the literature that are not industry adopted and well-established techniques.

In Virgili-Llop et al. (2019), the authors have proposed an optimal control approach for a spacecraft equipped with a robotic arm manipulator. Naturally, due to non-convexity nature arising from the nonlinear dynamics and the non-convex constraints, it is then proposed

a convexification approach to finding a locally optimal solution.

Resorting to well-established techniques from robust control, Rodrigues et al. (2022) presents a modeling technique based on Linear Fractional Transformation (LFT) for spacecraft that have flexible structures like solar panels or robotic arms. These LFT models can then be used in MPC controllers as was done in Relvas et al. (2022). It should be noted that robust control can also be complemented with guaranteed state estimation to detect faults, distinguish between modes of operation with respect to uncertain parameters and allow the refinement of the LFT model to the specific instance that the spacecraft state is in. In this context, the works in Silvestre et al. (2017b), Silvestre (2022c) and Silvestre et al. (2017a) have shown how to estimate the state for an uncertain Linear Parameter Varying (LPV) model, which can be extended for the LFT describing the spacecraft.

The paper Wijayatunga et al. (2023) introduces a MPC approach based on convex optimization to guide ADR missions. Convex optimization is capable of finding optimal solutions in polynomial time, but it typically requires successive convexification of nonconvex dynamics, which can introduce inaccuracies. In this work, the need for successive convexification is eliminated by utilizing near-linear Generalized Equinoctial Orbital Elements (GEqOE) and a novel split-Edelbaum approach for updating the reference trajectory. The solution accuracy is evaluated against a high-fidelity dynamics model, demonstrating that the MPC-convex method can produce precise solutions without the need for iterative processes.

## 6 Conclusions

This paper has comprehensively explored the crucial aspects of GNC systems for in-orbit servicing and assembly missions. The focus was placed on presenting the typical dynamical models used and the commonalities between far-range and close-range operations and how the different assumptions motivate simplifications in the differential equations. As a consequence, different proposals can be found in the literature for the two segments of the missions.

From the literature survey, two conclusions can be pointed out: i) the industry is rather conservative and missions have resorted to well-established techniques that have mathematical guaranteed of safety and operation; ii) there has been a considerable interest from the academic community in exploring optimization-based algorithms when applied to the IOS and IOA missions. The point ii) translated in various proposals focusing on the use of MPC that was typically used for industrial settings but is becoming more widespread in autonomous vehicles with the advent of cheap and compact processors. However, the same cannot be said for the space industry given that onboard processors are typically very limited in computing power due to the need of shielding and error correction to deal with the radiation in space.

Another interesting avenue of research that has been pursued is the use of QP problems where CLF and CBF can be used to ensure asymptotic stability and safety. These techniques promise very interesting advantages for the industry since these programs have closed-form solutions and have mathematical guarantees that are of prime importance to ensure viable solutions that do not compromise the high investment in space missions.

## Acknowledgments

This work was supported by the Portuguese Fundação para a Ciência e a Tecnologia (FCT) through project FirePuma (DOI: 10.54499/PCIF/MPG/0156/2019), through LARSyS FCT funding (DOI: 10.54499/LA/P/0083/2020, 10.54499/UIDP/50009/2020, and 10.54499/UIDB/50009/2020), through COPELABS, University Lusófona project UIDB/04111/2020, and by GMV.

## References

- Alazard D, Cumer C and Tantawi K (2008), Jun., Linear dynamic modeling of spacecraft with various flexible appendages and on-board angular momentums, Proceedings of the 7th International ESA Conference on Guidance, Navigation & Control Systems (GNC 2008), Tralee, County Kerry, Ireland, 1–14.
- Ankersen F, Wu SF, Aleshin A, Vankov A and Volochinov V (2005). Optimization of spacecraft thruster management function. *Journal of guidance, control, and dynamics* 28 (6): 1283–1290.
- Arney D, Sutherland R, Mulvaney J, Steinkoenig D, Stockdale C and Farley M. On-orbit Servicing, Assembly, and Manufacturing (OSAM) State of Play, 2021 Edition. White Paper 20210022660, OSAM National Initiative (2021). <https://ntrs.nasa.gov/citations/20210022660>.
- Bezerra JA and Santos DA (2021). Optimal exact control allocation for under-actuated multirotor aerial vehicles. *IEEE Control Systems Letters* 6: 1448–1453.
- Bonnal C, Ruault JM and Desjean MC (2013). Active debris removal: Recent progress and current trends. *Acta Astronautica* 85: 51–60. ISSN 0094-5765. doi:<https://doi.org/10.1016/j.actaastro.2012.11.009>. <https://www.sciencedirect.com/science/article/pii/S0094576512004602>.
- Boyd ID, Buenconsejo RS, Piskorz D, Lal B, Crane KW and Blanco EDL. On-Orbit Manufacturing and Assembly of Spacecraft. IDA Paper P-8335, IDA Science and Technology Policy Institute (2017). <https://www.ida.org/-/media/feature/publications/o/on/on-orbit-manufacturing-and-assembly-of-spacecraft/on-orbit-manufacturing-and-assembly-of-spacecraft.ashx>.
- Branco J, Colmenarejo P, Serra P, Lourenço P, Peters TV and Mammarella M (2021), Jun., Critical GNC Aspects for ADR missions, Proceedings of the 11th International ESA Conference on Guidance, Navigation & Control Systems, ESA, Virtual Event.
- Breeden J and Panagou D (2022). Guaranteed safe spacecraft docking with control barrier functions. *IEEE Control Systems Letters* 6: 2000–2005. doi:10.1109/LCSYS.2021.3136813.
- Briz J, Paulino N, Lourenço P, Cachim P, Forgues-Mayet E, Ferreira L, Groth A, Papadopoulos E, Rekleitis G, Nanos K and Preda V (2023),

- Sep., Guidance, Navigation, and Control of In-Orbit Assembly of Large Antennas – technologies and approach for IOANT, Proceedings of the 41st ESA Antenna Workshop on Large Deployable Antennas, ESA, Noordwijk, The Netherlands.
- Brown CD (1996a), Jan. Spacecraft Propulsion, American Institute of Aeronautics and Astronautics, Washington DC. ISBN 978-1-60086-244-1. doi:10.2514/4.862441.
- Brown CD (1996b). Spacecraft propulsion, AIAA, pp. 59.
- Carioscia SA, Corbin BA and Lal B. Roundtable Proceedings: Ways Forward for On-Orbit Servicing, Assembly, and Manufacturing (OSAM) of Spacecraft. IDA Document NS D-10445, IDA Science and Technology Policy Institute (2018). <https://www.ida.org/-/media/feature/publications/r/ro/roundtable-proceedings-ways-forward-for-on-orbit-servicing/d-10445.ashx>.
- Carter T and Briant J (1992). Fuel-optimal rendezvous for linearized equations of motion. *Journal of Guidance, Control, and Dynamics* 15 (6): 1411–1416. doi:10.2514/3.11404. <https://doi.org/10.2514/3.11404>.
- Chen D and Fujimoto K (2018). Rendezvous control of spacecraft via constrained optimal control using generating functions. *Transactions of the Japan Society for Aeronautical and Space Sciences, Aerospace Technology Japan* 16 (5): 392–397. doi:10.2322/tastj.16.392.
- Clohessy W and Wiltshire R (1960). Terminal guidance system for satellite rendezvous. *Journal of the Aerospace Sciences* 27 (9): 653–658.
- Colmenarejo P, Aida Alcalde Barahona, José Francisco Briz Valero, Peters TV, Dubanchet V, Henry D, Menon PP and Ankersen F (2018), Oct., Advanced GNC for In-Orbit Autonomous Assembly of Flexible Vehicles – IOA-GNC, Proceedings of the 69th International Astronautical Congress.
- Danielson C, Kloepfel J and Petersen C (2022). Spacecraft attitude control using the invariant-set motion-planner. *IEEE Control Systems Letters* 6: 1700–1705. doi:10.1109/LCSYS.2021.3132457.
- Dodge FT (2000). The New "Dynamic Behavior of Liquids in Moving Containers", Southwest Research Institute.
- Dong H, Hu Q and Akella MR (2017). Safety control for spacecraft autonomous rendezvous and docking under motion constraints. *Journal of Guidance, Control, and Dynamics* 40 (7): 1680–1692. doi:10.2514/1.G002322. <https://doi.org/10.2514/1.G002322>.
- Fehse W (2003), Nov. Automated Rendezvous and Docking of Spacecraft, Cambridge University Press. ISBN 978-1-139-44068-4.
- Flores-Abad A, Ma O, Pham K and Ulrich S (2014). A review of space robotics technologies for on-orbit servicing. *Progress in Aerospace Sciences* 68: 1–26. ISSN 0376-0421. doi:<https://doi.org/10.1016/j.paerosci.2014.03.002>. <https://www.sciencedirect.com/science/article/pii/S0376042114000347>.
- Fuller A, Fan Z, Day C and Barlow C (2020). Digital Twin: Enabling Technologies, Challenges and Open Research. *IEEE Access* 8: 108952–108971. ISSN 2169-3536. doi:10.1109/ACCESS.2020.2998358. <https://ieeexplore.ieee.org/document/9103025/>.
- Guffanti T and D'Amico S (2022), Robust passively safe spacecraft swarming via closed-form and optimization-based control approaches, 2022 American Control Conference (ACC), 416–423.
- Gurobi Optimization, LLC (2022). Gurobi Optimizer Reference Manual. <https://www.gurobi.com>.
- Koenig AW and D'Amico S (2021). Fast algorithm for fuel-optimal impulsive control of linear systems with time-varying cost. *IEEE Transactions on Automatic Control* 66 (9): 4029–4042. doi:10.1109/TAC.2020.3027804.
- Krejci D and Lozano P (2018). Space propulsion technology for small spacecraft. *Proceedings of the IEEE* 106 (3): 362–378. doi:10.1109/JPROC.2017.2778747.
- Li D, Zhong L, Zhu W, Xu Z, Tang Q and Zhan W (2022). A survey of space robotic technologies for on-orbit assembly. *Space: Science & Technology* 2022. doi:10.34133/2022/9849170. <https://spj.science.org/doi/pdf/10.34133/2022/9849170>. <https://spj.science.org/doi/abs/10.34133/2022/9849170>.
- Lizy-Destrez S, Le Bihan B, Campolo A and Manglativi S (2017), Sep., Safety Analysis for Near Rectilinear Orbit Close Approach Rendezvous in the Circular Restricted Three-Body Problem, The 68th annual International Astronautical Congress (IAC 2017), Adelaide, Australia, <https://hal.science/hal-01755252>.
- Malyuta D and Açikmeşe B (2020). Lossless convexification of optimal control problems with semi-continuous inputs. *IFAC-PapersOnLine* 53 (2): 6843–6850.
- Misra G and Bai X (2020). Iteratively feasible optimal spacecraft guidance with non-convex path constraints using convex optimization, AIAA. doi:10.2514/6.2020-1350. <https://arc.aiaa.org/doi/pdf/10.2514/6.2020-1350>, <https://arc.aiaa.org/doi/abs/10.2514/6.2020-1350>.
- Pesce V, Colagrossi A and Silvestrini S, (Eds.) (2022). Modern Spacecraft Guidance, Navigation, and Control: From System Modeling to AI and Innovative Applications, Elsevier. ISBN 978-0-323-90917-4.
- Reis MF, Aguiar AP and Tabuada P (2021). Control barrier function-based quadratic programs introduce undesirable asymptotically stable equilibria. *IEEE Control Systems Letters* 5 (2): 731–736. doi:10.1109/LCSYS.2020.3004797.
- Relvas M, Lourenço P and Batista P (2022), Nonlinear mpc for attitude guidance & control of autonomous spacecraft, Brito Palma L, Neves-Silva R and Gomes L, (Eds.), CONTROL 2022, Springer International Publishing, Cham, 15–25.
- Roa Garzon MA, Nottensteiner K, Grunwald G, Lopez P, Cuffolo A, Andiappane S, Rognant M, Verghaeghe A and Bissonnette V (2019), May, In-space robotic assembly of large telescopes, Symposium on Advanced Space Technologies in Robotics and Automation - ASTRA, ESA, <https://elib.dlr.de/133673/>.
- Rodrigues R, Preda V, Sanfedino F and Alazard D (2022). Modeling, robust control synthesis and worst-case analysis for an on-orbit servicing mission with large flexible spacecraft. *Aerospace Science and Technology* 129: 107865. ISSN 1270-9638. doi:<https://doi.org/10.1016/j.ast.2022.107865>. <https://www.sciencedirect.com/science/article/pii/S1270963822005399>.
- Serra P, Lourenço P, Branco J, Briz Valero JF, Mammarella M, Peters TV, Manara S, Bernardini D, Bemporad A, Manzillo P, Witteveen J and Cropp A (2021), Jun., Computational Guidance & Navigation for Bearings-Only Rendezvous – methods and outcomes of GUIBEAR, Proceedings of the 11th International ESA Conference on Guidance, Navigation & Control Systems, ESA, Virtual Event.
- Sidi MJ (1997). Spacecraft Dynamics and Control: A Practical Engineering Approach, Cambridge Aerospace Series, Cambridge University Press, Cambridge. ISBN 978-0-521-78780-2. doi:10.1017/CBO9780511815652. <https://www.cambridge.org/core/books/spacecraft-dynamics-and-control/E9CAEE81CD09527C99497FA8C7C35B0A>.
- Silvestre D (2022a), Accurate guaranteed state estimation for uncertain lps using constrained convex generators, 2022 IEEE 61st Conference on Decision and Control (CDC), 4957–4962.
- Silvestre D (2022b). Constrained convex generators: A tool suitable for set-based estimation with range and bearing measurements. *IEEE Control Systems Letters* 6: 1610–1615. doi:10.1109/LCSYS.2021.3129729.
- Silvestre D (2022c). Set-valued estimators for uncertain linear parameter-varying systems. *Systems & Control Letters* 166: 105311. ISSN 0167-6911. doi:<https://doi.org/10.1016/j.sysconle.2022.105311>. <https://www.sciencedirect.com/science/article/pii/S0167691122001141>.
- Silvestre D (2023). Exact set-valued estimation using constrained convex generators for uncertain linear systems. *IFAC-PapersOnLine* 56 (2): 9461–9466. ISSN 2405-8963. doi:<https://doi.org/10.1016/j.ifacol.2023.10.241>. 22nd IFAC World Congress, <https://www.sciencedirect.com/science/article/pii/S240589632300592X>.
- Silvestre D and Ramos G (2023). Model predictive control with collision avoidance for unknown environment. *IEEE Control Systems Letters* 7:

- 2821–2826. doi:10.1109/LCSYS.2023.3288884.
- Silvestre D, Rosa P, Hespanha JP and Silvestre C (2017a). Set-based fault detection and isolation for detectable linear parameter-varying systems. *International Journal of Robust and Nonlinear Control* 27 (18): 4381–4397. doi:<https://doi.org/10.1002/rnc.3814>. <https://onlinelibrary.wiley.com/doi/pdf/10.1002/rnc.3814>, <https://onlinelibrary.wiley.com/doi/abs/10.1002/rnc.3814>.
- Silvestre D, Rosa P, Hespanha JP and Silvestre C (2017b). Stochastic and deterministic fault detection for randomized gossip algorithms. *Automatica* 78: 46–60. ISSN 0005-1098. doi:<https://doi.org/10.1016/j.automatica.2016.12.011>. <https://www.sciencedirect.com/science/article/pii/S0005109816305192>.
- Taborda P, Matias H, Silvestre D and Lourenço P (2024). Convex mpc and thrust allocation with deadband for spacecraft rendezvous. *IEEE Control Systems Letters* : 1–1doi:10.1109/LCSYS.2024.3407611.
- Tatsch A, Fitz-Coy N and Gladun S (2006), On-orbit servicing: A brief survey, IEEE International Workshop on Safety, Security, and Rescue Robotics (SSRR'06), New York.
- Underwood C, Pellegrino S, Lappas VJ, Bridges CP and Baker J (2015). Using cubesat/micro-satellite technology to demonstrate the autonomous assembly of a reconfigurable space telescope (aarest). *Acta Astronautica* 114: 112–122. ISSN 0094-5765. doi:<https://doi.org/10.1016/j.actaastro.2015.04.008>. <https://www.sciencedirect.com/science/article/pii/S0094576515001642>.
- Virgili-Llop J, Zagaris C, Richard Zappulla I, Bradstreet A and Romano M (2019). A convex-programming-based guidance algorithm to capture a tumbling object on orbit using a spacecraft equipped with a robotic manipulator. *The International Journal of Robotics Research* 38 (1): 40–72. doi:10.1177/0278364918804660. <https://doi.org/10.1177/0278364918804660>.
- Weiss A, Baldwin M, Erwin RS and Kolmanovsky I (2015). Model predictive control for spacecraft rendezvous and docking: Strategies for handling constraints and case studies. *IEEE Transactions on Control Systems Technology* 23 (4): 1638–1647. doi:10.1109/TCST.2014.2379639.
- Wertz JR, Everett DF and Puschell JJ (2011). *Space Mission Engineering: The New SMAD*, first ed., Space Technology Library, 28, Microcosm Press. ISBN 978-1-881883-15-9.
- Wie B (2008). *Space Vehicle Dynamics and Control*, second edition ed., American Institute of Aeronautics and Astronautics, Reston ,VA. ISBN 978-1-56347-953-3. doi:10.2514/4.860119. <https://arc.aiaa.org/doi/abs/10.2514/4.860119>.
- Wijayatunga M, Armellin R, Holt H, Pirovano L and Bombardelli C (2023). Convex optimization-based model predictive control for the guidance of active debris removal transfers. 2308.08783, <https://arxiv.org/abs/2308.08783>.
- Yang Y (2018), Aug. Coupled orbital and attitude control in spacecraft rendezvous and soft docking. *Proceedings of the Institution of Mechanical Engineers, Part G: Journal of Aerospace Engineering* 233 (9): 3109–3119. ISSN 2041-3025. doi:10.1177/0954410018792991. <http://dx.doi.org/10.1177/0954410018792991>.
- Yang Y (2019), Feb. *Spacecraft Modeling, Attitude Determination, and Control: Quaternion-Based Approach*, CRC Press. ISBN 978-0-429-82214-8.